Vol. 692: 99–118, 2022 https://doi.org/10.3354/meps14071

MARINE ECOLOGY PROGRESS SERIES Mar Ecol Prog Ser

Published June 30



Characterization and spatial variation of the deep-sea fish assemblages on Pioneer Bank, Northwestern Hawaiian Islands

Beatriz E. Mejía-Mercado, Amy R. Baco*

Department of Earth, Ocean and Atmospheric Science, Florida State University, EOAS Building, 1011 Academic Way, Tallahassee, Florida 32306, USA

ABSTRACT: Knowledge of the spatial variation of deep-sea fish assemblages is a critical gap in understanding seamount ecology. Pioneer Bank in the Papahānaumokuākea Marine National Monument (Hawaii, USA) has a history of hook-and-line fishing but not trawling; thus, it is a good location to further describe deep-sea fish assemblages. From replicated autonomous underwater vehicle transects at 300, 450, and 600 m on 3 sides of Pioneer Bank, we observed 4190 fish representing 81 species. Fish assemblages were dominated by Gadiformes, Perciformes, and Stomiiformes. The relative abundance of fish was significantly different among sides of the seamount and the interaction of side and depth, with the NW side having the highest relative abundance at 450 m. Species richness, rarefaction estimates of expected species richness, Shannon diversity, and Simpson dominance showed significant differences by side, but not by depth. These differences were between the S and NW sides, with the S side having the lowest diversity and high dominance. The structure of the fish assemblage was significantly different among both sides and depths, with depth as the most important factor. Fish assemblage structure was most strongly correlated with salinity, % rugosity, chlorophyll a, and mean direction of substrate. These scales of spatial variability both with depth and across short horizontal distances on a single seamount are similar to those found on nearby Necker Island, which reaffirms the spatial heterogeneity in deepsea fish assemblages on seamounts. This study provides an ecological baseline for the management and conservation of seamounts.

KEY WORDS: Fish community structure · Seamounts · Papahānaumokuākea Marine National Monument · Patterns of distribution

- Resale or republication not permitted without written consent of the publisher

1. INTRODUCTION

Knowledge of deep-sea fish assemblages and their spatial variation is a critical gap in understanding seamount ecology and is relevant for designing deep-sea protected areas. Seamounts, including banks and oceanic islands (Staudigel & Clague 2010), harbor a high diversity and abundance of deep-sea species (Mundy 2005, Samadi et al. 2006, Rowden et al. 2010). Deep-sea corals and sponges are usually the most abundant taxa in number and biomass (Rogers 1994,

Samadi et al. 2007). These species support a diverse community of other organisms, including deep-sea fishes (Husebo et al. 2002, Milligan et al. 2016, Devine et al. 2020), that are important for maintaining ecosystem balance.

Seamounts are also heterogeneous habitats with different physical, chemical, and geological conditions that influence spatial variation in community structure. Due in part to this heterogeneity, the abundance and diversity of species on seamounts appear to vary from one seamount to another (e.g. Tracey et

al. 2004, 2012, McClain 2007, Morato & Clark 2007, Clark et al. 2010b, 2012, Rowden et al. 2010, Mejía-Mercado et al. 2019). Variation in abundance might be influenced by the interaction of flow characteristics, such as Taylor columns (Rogers 1994), and topographic characteristics that together influence the flux of organic materials toward the seafloor and their retention on the substrate (White et al. 2007). Variation in the diversity of species might be influenced by water mass characteristics such as temperature, dissolved oxygen, salinity, and density (Koslow et al. 1994, Clark et al. 2010a, Tracey et al. 2012, Mejía-Mercado et al. 2019).

Increasingly, evidence for spatial variation in benthic invertebrate communities within single seamounts has been found both vertically and horizontally (e.g. Bo et al. 2011, Long & Baco 2014, Morgan et al. 2015, Victorero et al. 2018). However, the spatial variation of fishes within a single seamount has not received significant attention, with only a few recent studies (e.g. Mejía-Mercado et al. 2019, Leitner et al. 2021). A recent study of Necker Island, a seamount in the Northwestern Hawaiian Islands (NWHI), USA, suggests that fishes may show similar levels of spatial variation to benthic invertebrates, with differences in fish assemblage structure by depth and side of the seamount (Mejía-Mercado et al. 2019). On a vertical scale, depth, in correlation with temperature and dissolved oxygen, plays an important role in the distribution of fish species based on their biological and physiological characteristics (Thistle 2003, Clark et al. 2010b). On a horizontal scale, topography and the type of substratum that characterize a specific location on a seamount may influence species composition due to habitat preferences. Similarly, oceanographic conditions can interact with the geology of the area and alter the availability of food supply that regulates the abundance of organisms by location (Boehlert & Genin 1987, Rogers 1994, Genin 2004, Clark et al. 2010b).

As new evidence for spatial variability in seamount fish assemblages emerges, it becomes important to document these patterns, ideally at undisturbed locations, to understand the scales of variation and to recognize environmental variables that relate to the observed patterns. The islands and seamounts of the NWHI are currently protected from fishing as part of the Papahānaumokuākea Marine National Monument (PMNM), with a protection history of approximately 110 yr (NOAA Office of National Marine Sanctuaries 2020). Since 1909, all of the NWHI except Midway Atoll were established as the Hawaiian Islands Bird Reservation, renamed in 1940 as the

Hawaiian Islands National Wildlife Refuge. In 1976, the State of Hawaii, US Fish and Wildlife Service, and NOAA Fisheries began working together to provide a baseline for the ecological status of the NWHI. In 2000, the NWHI was designated a Coral Reef Ecosystem Reserve, and in 2006, it became a Marine National Monument, later renamed the PMNM. In 2010, the PMNM was established as a World Heritage site under the United Nations World Heritage Convention, a designation that allowed the protection of the cultural and ecological heritage of the Monument. Finally, in 2016, the Monument was extended to 4 times the initial size (Kikiloi et al. 2017), which currently makes it the world's third-largest protected area (terrestrial or marine). Despite all of this protection history, there is still a lack of information about the organisms inhabiting most NWHI seamounts. A greater understanding of the taxonomy and ecological patterns of these organisms can be used to improve the management and conservation of the region (Kennedy et al. 2019).

The spatial variation of fishes on Necker Island, a seamount located in the PMNM, was recently studied on 3 sides at 50 m depth intervals from 200 to 700 m (Mejía-Mercado et al. 2019). Using autonomous underwater vehicle (AUV) photos, 92 species were identified on Necker, with 25 records of species new to this seamount and 4 new to the Hawaiian Archipelago. The fish assemblages were dominated by Stomiiformes, Gadiformes, Myctophiformes, Aulopiformes, and Perciformes, and their abundance varied significantly by side of the seamount and by depth. Species richness and community structure varied by side, depth, and the interaction of both factors. Mejía-Mercado et al. (2019) also observed that variability in the community structure was driven by dissolved oxygen (and its correlate temperature), salinity, % sand (and its correlate substrate size), rugosity, slope, particulate organic carbon (POC) (and its correlate chlorophyll a [chl a]), and surface current vectors u (east–west) and v (north–south).

The NWHI covers a large geographic area. Therefore, it is important to know if the results obtained on one protected seamount are comparable to the patterns on other protected seamounts in the same region. This study focuses on Pioneer Bank, another seamount located in the PMNM. This bank is an example of a site with little information on the occurrence and distribution of deep-sea fish species (Uchida & Uchiyama 1986, Parrish & Boland 2004, Mundy 2005, Daly-Engel et al. 2018) and a lack of information on the ecology of fish communities. In addition, Pioneer Bank has a history of hook-and-line

fishing for deepwater snappers and groupers (Haight et al. 1993) but not trawling, making it a good location to describe spatial variation in deep-sea fish assemblages in the absence of anthropogenic impacts, and to explore the relationship of this spatial variabil-

ity with environmental variables. The goal of this study was to describe the composition, diversity, and abundance of the deep-sea fish fauna on Pioneer Bank. Based on observations on Necker Island, the hypothesis was tested that deep-sea fish assemblages would vary with seamount side and depth. An additional objective was to determine which environmental variables were correlated with the observed assemblage structure.

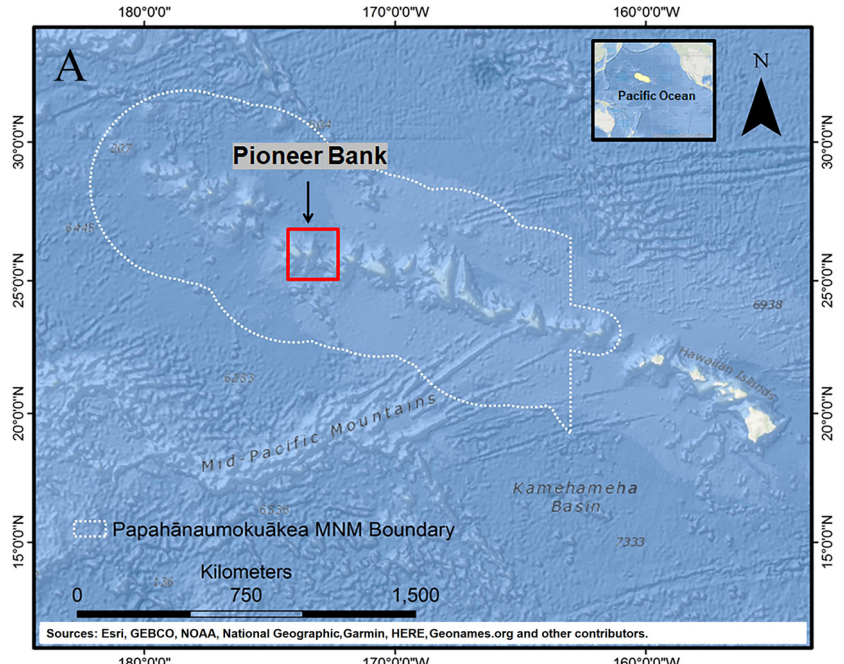
2. MATERIALS AND METHODS

2.1. Study area and data collection

Pioneer Bank (26° 00′ N, 173° 25′ W; Fig. 1A) is a seamount in the NWHI located east of Lisianski Island, about 1670 km from Honolulu, 920 km from Necker Island, and 450 km southwest of Midway Atoll. From northeast to southwest, the summit measures close to 29 km, and from northwest to southeast close to 21 km. Its shallowest depth is 31 m (Uchida & Uchiyama 1986), and the shelf area from this depth to 90 m deep is about 312 km² (Parrish & Boland 2004).

AUV surveys were conducted as a part of a project examining the recovery of deep-sea coral communities impacted by trawling in the NWHI, with this site included as a 'never trawled' control (Baco et al. 2019, 2020). Images were collected using the AUV 'Sentry' (National Deep Submergence Facility, https://ndsf.whoi.edu/sentry/), deployed on Pioneer Bank from the RV 'Kilo Moana' in 2014 (on the NW and S sides of the bank) and 2015 (on the NE side) (Table 1). For each side, 2-3 replicate photo transects, with a length of ~1000 m, were carried out at 300, 450, and 600 m along the depth contour (Fig. 1B). These depths were chosen

based on the fish assemblage changeover on nearby Necker Island (Mejía-Mercado et al. 2019). The AUV moved at speeds of 0.5–0.7 m s⁻¹ with an altitude off the bottom between 4 and 8 m (average of 5 m). Detailed data by transect are available in Table S1 in



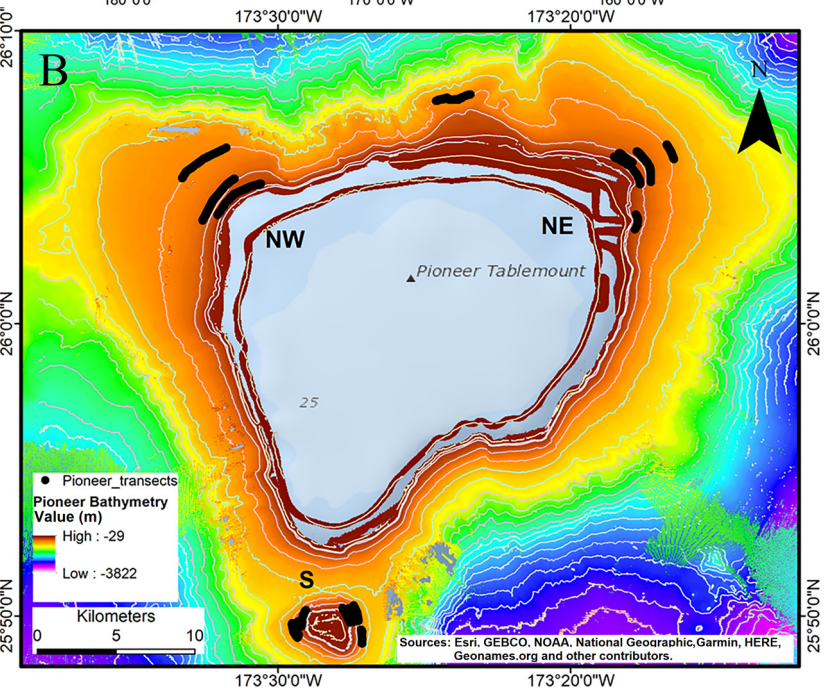


Fig. 1. (A) Hawaiian Archipelago showing the Papahānaumokuākea Marine National Monument indicated by the white line and Pioneer Bank by the red box. (B) Bathymetric map of Pioneer Bank using combined 40 and 50 m resolution multibeam data. Autonomous underwater vehicle (AUV) dive tracks are indicated by the thick black lines in the NW, S, and NE sides. Maps were created in ArcMap 10.4.1 (Esri 2016)

Table 1. Location of autonomous underwater vehicle (AUV) dives on Pioneer Bank, Northwestern Hawaiian Islands. On each side, 2–3 replicate transects of 1000 m were surveyed along depth contours at each of 300, 450, and 600 m

Side	AUV 'Sentry' dive No.	Year sampled	Mean latitude (° N)	Mean longitude (° W)	No. of transects
NW	S288	2014	26.082	173.530	9
S	S289	2014	25.834	173.470	7
NE	S357	2015	26.099	173.314	9

Supplement 1 at www.int-res.com/articles/suppl/m692 p099_supp1.xlsx. A down-looking Allied Vision Technologies Prosilica GE4000C camera mounted on the AUV was used to take photos every 3-4 s with a resolution of 96 dpi (4008×2672 pixels) and a field of view of approximately 12 m^2 .

2.2. Photo analysis

AUV images were scanned for the presence of benthic and demersal fishes on a 24 in (60.96 cm) computer monitor following the methodology applied by Mejía-Mercado et al. (2019). Fish of 3 cm in length could be resolved and were taxonomically identified by B. Mejía-Mercado based on Carpenter & Niem (1998, 1999a,b, 2001a,b), Chave & Malahoff (1998), Mundy (2005), Randall (2007), and Nelson et al. (2016), as well as unpublished notes on the identification of fishes in the Hawaiian biogeographic region compiled by collaborator Bruce Mundy, who also corroborated these identifications. To be conservative in taxonomic identification, following Mejía-Mercado et al. (2019), each identification was scored with a confidence number on a scale of 1-4, where (1) was certainty in the putative taxon or genus, (2) certainty in the family, (3) certainty in the order, and (4) certainty in the class. Putative species identified with this approach were subsequently referred to as 'species' for simplicity. All organisms were counted and included in descriptive statistics, while only those with a confidence number of 1 were used for univariate and multivariate analyses. The number of individuals per transect was divided by the number of photos successfully analyzed in that transect to obtain standardized values for comparisons among transects.

2.3. Environmental data

Seafloor bathymetry and acoustic backscatter data with 20 m resolution were obtained using a Kongs-

berg EM122 Multibeam Echosounder on the RV 'Kilo Moana.' This bathymetry was complemented with 50 m resolution data extracted online from NOAA (2019) because it did not cover the entire surveyed area on the slopes. Sonar files were cleaned using Qimera 3D editor, and the raster grid files were constructed in Fledermaus (QPS software). The contours were derived in ArcGIS 10.4.1 (Esri 2016) from these data, and used with the bathy-

metric data to create the map of the bank (Fig. 1B).

Both the AUV ultra-short baseline tracking and the ship's GPS tracking were used to map each transect in ArcGIS 10.0 using XY layers. The length of each transect was obtained using the 'Geospatial Modeling Environment' package for R (Beyer 2012). The aspect of the substrate, which was used to derive mean direction of the substrate (or direction of the slope), was computed from the sine and cosine layers created from the original aspect raster by using the Map Algebra function within ArcView (Long & Baco 2014). These circular data were then used in the equations defined by Fisher (1995) to be converted into mean direction of the substrate, linear data that can be used for DistLM analyses.

Dissolved oxygen was obtained in situ with a sensor (Aanderaa optode, model 4330, accuracy <1 μ) attached to the AUV 'Sentry.' Conductivity, temperature, and depth were obtained with a Seabird SBE49 CTD with a Seapoint optical backscatter sensor. Conductivity and temperature accuracy were 0.0003 S m^{-1} and 0.002°C. The position was derived from an ultrashort baseline (USBL) and a Doppler velocity log (DVL) dead reckoning. Accuracy varied depending on depth, but the DVL accuracy was on a cm scale, and the USBL accuracy was on the order of 5–10 m. Each measurement was time-stamped to match each image at the time of image capture. Salinity was converted from conductivity in MATLAB using an algorithm created by Fofonoff & Millard (1983).

POC, surface chl *a*, and surface current vectors were obtained from Baco et al. (2017). Briefly, POC and chl *a* were extracted from the National Oceanic and Atmospheric Administration's Environmental Research Division's Data Access Program (ERDDAP) Data Set (Simons 2011). POC and monthly values of surface chl *a* with 4 km resolution were extracted from the NESDIS satellite using data from the Visible Infrared Imager/Radiometer Suite (VIIRS) (https://coastwatch.pfeg.noaa.gov/erddap/griddap/nesdis VHNSQchlaDaily.html), and monthly values of surface chl *a* with 0.025 degree resolution were derived

from the Aqua-MODIS satellite (https://coastwatch.pfeg.noaa.gov/erddap/griddap/erdMBchla1day_Lon PM180.html). All of these parameters were extracted from January 2008 to December 2016. Surface current vectors u (east—west) and v (north—south) were obtained from the Hybrid Coordinate Ocean Model (HYCOM) with 1/12 degree resolution from 1 January 2015 to 1 January 2016 for the NE side and from 1 January 2014 to 1 January 2015, for the NW and S sides of the bank. The visualization of these data (*. NetCDF) was made in Matlab, and the average values were calculated in ArcMap 10.4.1 (Esri 2016).

The characteristics of the substrate were defined for each transect based on a categorical scale (Table 2) in every fourth photo achieving a resolution of 3–4 m. Substrate composition and substrate size were obtained using the point-count method that consisted of 15 random points drawn on each photo using Image J software (e.g. Mortensen & Buhl-Mortensen 2004, Mejía-Mercado et al. 2019). Rugosity, defined as the roughness of the seafloor, and slope were estimated for the entire photo. Substrate composition was converted to the percentage (%) of sand, and substrate size was expressed as a phi value. Rugosity was expressed as the percentage of smooth surface and slope as the percentage of flat slope (0–50°). The

Table 2. Characteristics of the substrate described for each transect on Pioneer Bank at 300, 450, and 600 m depth. Substrate composition and size were estimated in 15 random points within each analyzed photo, whereas rugosity and slope were described for the entire photo

Substrate composition	(WS) (C)	Manganese or basalt White sand Carbonate Coral rubble
Grain size (phi value)	(-3) (-4) (-7) (-10) (-12)	Sand Pebble Coral rubble Cobble Boulder Outcrop Hardpan
Rugosity	` '	Smooth surface Low – little folding/roughness Medium – intermediate complexity and roughness Coral Rubble – sharp jagged rubble with several layers High – very rough and complex surface, generally large relief
Slope	(1) (2) (3) (4)	Flat: 0–50°

number of points from each transect for each substrate size was counted by each category, multiplied by a phi value using the scale described by Blair & McPherson (1999), with a hardpan phi value addition, and divided by the number of photos in the transect. This conversion allowed us to obtain a numeric variable for grain size.

All environmental data collected on Pioneer Bank and the average for each transect at each seamount side are summarized in Table S1.

2.4. Statistical analyses

The sampling effort was evaluated using species accumulation curves with the observed and expected species (Chao 2, Jackknife 1, and Jackknife 2). The curves were constructed with 10 000 randomizations.

Spatial variation in deep-sea fishes was assessed using relative abundance (individuals / no. of photos), species richness (S), rarefaction estimates of the expected species richness in a sample of 300 individuals ($E_{S(300)}$), and Shannon diversity (H', natural digits) and Simpson dominance (D) indices. These attributes were compared among survey locations using Euclidean distance matrices in a 2-way crossed ANOVA with 2 factors: seamount side (NW, S, and NE) and depth (300, 450, and 600 m). Pairwise tests were constructed with 10 000 residual permutations under model III and Monte Carlo (MC) tests due to the low number of permutations (Anderson et al. 2008). Results were considered significant at p \leq 0.05.

Differences in the deep-sea fish assemblage structure were tested using a permutational multivariate analysis of variance (PERMANOVA), constructed with the fourth-root transformed relative abundance, Bray-Curtis similarity matrix (Clarke & Warwick 2001), and testing with 10 000 residual permutations. Initially, we used the Bartlett test for homogeneity and plotted the data to see their distribution and test for normality. The data without transformation did not meet the assumptions of homogeneity and normality. We therefore used fourth-root transformation and tested again for assumptions of normality and homogeneity of variances (for parametric tests). The transformed data did meet homogeneity but not normality. With these results, we applied permutations with a PERMANOVA test, which is a non-parametric test and should not be affected by deviations from normality. The fourth-root transformation (intermediate-level) decreases the contribution of highly abundant species and increases the contribution of less abundant species (Clarke & Warwick 2001). Differences in fish assemblage structure were tested with the 2-way crossed model with seamount side and depth as fixed factors as described above, and results were again considered significant at $p \le 0.05$.

Non-metric multidimensional scaling (NMDS) ordination, based on the Bray-Curtis similarity matrix, was used to observe the similarities in community structure among transects, by sides and depth. To corroborate the results in the NMDS ordination, a dendrogram of transects produced by hierarchical clustering and group average was used, using SIM-PROF analyses to test for any significant differences between clusters. Contributions of individual species to the dissimilarity and similarity among the *a posteriori* groups formed from the above analyses were determined using a 1-way similarity percentage (SIMPER) analysis based on the Bray-Curtis similarity matrix and with a 50% cut-off (Clarke & Warwick 2001).

To visualize variability in the environmental variables (temperature, salinity, dissolved oxygen, mean direction of substrate, % sand, % rugosity, grain size, % slope, POC, chl a [extracted from MODIS and NES-DIS], vectors of currents u and v, and time of day) among transects, a principal components analysis (PCA) was used with these variables averaged by transect. Variables were normalized and analyzed with draftsman plots to look for highly correlated pairs with an absolute value of $r \ge 0.90$ (Clarke & Warwick 2001), from which one of the pair of variables was removed as was the case between temperature and oxygen and current vectors v and u (Table S2 in Supplement 1). Multicollinearity was then tested among the remaining variables, removing them one by one, starting from the variable with the highest collinearity and leaving only those variables with a variance inflation factor (VIF) <5 (Chatterjee et al. 2000, Zuur et al. 2010). Correlation between environmental variables and community structure was evaluated with salinity, mean direction of the substrate, % slope, % rugosity, grain size, chl a extracted from NESDIS, current vector v, and time of day. The most important environmental variables correlated with the observed community structure patterns were obtained using distancebased linear modeling (DistLM, Anderson et al. 2008) combined with Akaike's information criterion (AIC, Akaike 1973), and the best procedure that considers the value of the AIC for all potential combinations of predictor variables (Anderson et al. 2008). Distancebased redundancy (dbRDA) and NMDS bubble plots allowed us to illustrate the relationship between the most important variables as defined by DistLM and the structure of the assemblages. All statistical analyses and calculations of diversity indices were performed using PRIMER V6 + PERMANOVA software (Anderson et al. 2008), and the VIF was determined using the 'vegan' package (Oksanen et al. 2010) in RStudio v. 1.2.5042 (RStudio Team).

3. RESULTS

3.1. Deep-sea fish assemblage abundance and composition

In 12387 photos taken on 3 sides of Pioneer Bank covering a total area of approximately 110810 m², a total of 4190 individual fish were observed with a size range of approximately 3 cm to 2 m. Of these, 3440 (82.1%) individuals with a 1, 2, or 3 taxonomic certainty were identified in 23 orders with 42 families of bony fishes and 2 orders with 3 families of cartilaginous fishes (Table 3). The highest abundance of individuals occurred in the order Gadiformes (23.5%) with a strong representation by Macrouridae (Fig. 2A). This order was most common on the NW side at 600 m (Fig. 2B). Perciformes were the most diverse order and the next most common at 16.8%, with Symphysanodontidae having the highest abundance in the order (Fig. 2A) and occurring most commonly on the NE side and at 300 m (Fig. 2B,C). Stomiiformes (14.9%) were only represented by Sternoptychidae (Fig. 2A), the most abundant family overall, with high abundance on the NE side at 300 m (Fig. 2B). Scorpaeniformes, Myctophiformes, and 20 other orders were each below 10% of individuals. Sharks were represented by the orders Squaliformes and Carcharhiniformes with 3 families (Table 3).

We identified 81 species, of which some had not been previously described for Pioneer Bank but had been described for other seamounts in the NWHI. Species accumulation curves suggested that these 81 species identified on Pioneer Bank represented 73–80% of the species richness expected for the studied area. Jackknife 2 resulted in a maximum expected richness of 111, while Chao 2 and Jackknife 1 showed a slightly lower value (101) (Fig. S1 in Supplement 2 at www.int-res.com/articles/suppl/m692p099_supp2.pdf).

3.2. Spatial variation

Relative abundance showed significant differences among sides (p = 0.016) with an interaction with depth (p = 0.024) (Table 4). Based on the pairwise

Table 3. Composition and number of individuals of deep-sea fishes observed on 3 sides (NW, S, and NE) on Pioneer Bank and at the 3 sampled depths. The taxonomic classification follows Nelson et al. (2016), and new records for Pioneer Bank are indicated with an asterisk

Order	Family	Species	Side NW S		Total		(m) 600	
Class Chondrichthy	es							
Carcharhiniformes	Pseudotriakidae	Pseudotriakis microdon*		1	1			1
Squaliformes	Centrophoridae Squalidae	Centrophorus sp.* Squalus hawaiiensis	3 2 23	3 15	8 38	2 32	3 6	3
Class Osteichthyes Anguilliformes	Congridae	Ariosoma marginatum Ariosoma sp. Gnathophis cf. heterognathos*	1 30	1 11 11	1 12 41	1 37	3 4	1 8
	Nettastomatidae	Nettastoma parviceps*	6 1	5	12	1	6	5
	Ophichthidae	Ophichthidae Ophichthidae sp. 1	1		1 1	1	1	
	Synaphobranchidae	Synaphobranchidae Ilyophis sp. 1* Synaphobranchus sp. 1	2 2 7 1	1	2 10 1	1	9	
Argentiniformes	Argentinidae	Glossanodon struhsakeri	1 7	43	51	44	7	
Stomiiformes	Sternoptychidae	Argyripnus sp.	118 93	303	514	411	103	
Ateleopodiformes	Ateleopodidae	Ijimaia plicatellus*	2	1	3			3
Aulopiformes	Chlorophthalmidae	Chlorophthalmus proridens	95	35	130	3	36	91
Myctophiformes	Neoscopelidae	Neoscopelus macrolepidotus	20 46	140	206	28	2	176
Polymixiiformes	Polymixiidae	Polymixia nobilis	40 17		57	4	42	11
Zeiformes	Parazenidae	Stethopristes eos	4 8	4	16			16
	Zeidae	Zenopsis nebulosa	1		1		1	
	Zeniontidae	Cyttomimus stelgis	1 10		11		3	8
Gadiformes		Gadiformes	80 49	25	154	103	39	12
	Macrouridae	Macrouridae	16 13	18	47			27
		Coelorinchus aratrum*	17 6	4	27		89	5
		Coelorinchus gladius* Coelorinchus tokiensis*	74 5 7	15 1	94 8		2	6 15
		Hymenocephalus antraeus*	2 2	11	15			3
		Hymenocephalus sp. 1		3	3	5	9	33
		Macrouridae sp. 5 Malacocephalus cf. hawaiiensis*	107 9	14 56	14 172	7	84	14 81
		Pseudocetonurus septifer*	107 5	2	2	,	04	2
		Ventrifossa atherodon*	11 4	43	58	1	6	51
	Moridae	Moridae	22 28	10	60	2	40	
		Laemonema rhodochir Laemonema sp.	9 13 8 21	20 43	42 72	58 45	14 14	1
		Physiculus grinnelli	4	8	12	40	17	12
		Physiculus nigripinnis*	7 10	10	27	18	1	8
Holocentriformes	Holocentridae	Pristilepis oligolepis	2		2	2		
Trachichthyiformes	Trachichthyidae	Hoplostethus crassispinus*	40	2	42	3		39
Beryciformes	Berycidae	Berycidae	6		6			6
		Beryx decadactylus	6	0	6	2	3	1
Ombidiifo	Caranidas	Beryx splendens	5 51	3	59 7	8	3	48
Ophidiiformes	Carapidae	Pyramodon ventralis Ophidion muraopolopis*	2 3	2	7 3	7 3		
	Ophidiidae	Ophidion muraenolepis*	ა		ა	ى -		

Table continues on next page

Table 3 (continued)

Order	Family	Species		Sides NW S NE			Depth (m) 300 450 600		
Carangiformes	Carangidae	Decapterus sp. Seriola dumerili			1 9	1 9	9	1	
Pleuronectiformes		Pleuronectiformes	3			3			3
	Bothidae	Bothidae Bothidae sp. 1 Bothidae sp. 2 Chascanopsetta crumenalis* Chascanopsetta prorigera Parabothus cf. coarctatus Taeniopsetta radula	2 4 12		6 1 4 11 16 3 4	8 1 4 15 28 3 4	1 1 4 4 3 4	16	7 15 8
	Cynoglossidae	Symphurus strictus*	14		120	134	-		134
Callionymiformes	Callionymidae	Synchiropus sp.			1	1		1	
Scombriformes	Gempylidae	Rexea nakamurai*	2	21	2	25	7	1	17
Scomornornics	Trichiuridae	Benthodesmus cf. tenuis	-	1	-	1	,	-	1
Trachiniformes	Percophidae	Chrionema chryseres* Chrionema squamiceps*	27 14	76	48 5	151 19	65 16	86 3	1
	Pinguipedidae	Parapercis roseoviridis			8	8	8		
Labriformes	Labridae	Bodianus sanguineus*			1	1	1		
Perciformes		Perciformes			21	21	19		2
	Epigonidae	Epigonidae Epigonus cf. glossodontus* Epigonus devaneyi*		19	1 5 1	20 5 1	1	19	5 1
	Lutjanidae	Lutjanidae Etelis carbunculus Etelis coruscans Pristipomoides filamentosus	1	3	86 12 2 75	86 15 2 84	86 15 2 1	81	2
	Pentacerotidae	Pentaceros wheeleri	1			1		1	
	Serranidae	Liopropoma maculatum* Plectranthias kelloggi			1 10	1 10	1 9	1	
	Symphysanodontidae	Symphysanodon maunaloae	41	4	288	333	258	75	
Scorpaeniformes	Bembridae	Bembradium roseum	75	18	17	110	63	47	
	Hoplichthyidae Peristediidae	Hoplichthys citrinus Scalicus engyceros Scalicus hians	1 40 15	5	14 26 20	15 71 35	12 3	3 56	12 35
	Scorpaenidae	Scorpaenidae Pontinus macrocephalus Scorpaena pele* Scorpaenidae sp. 6 Scorpaenidae sp. 7 Scorpaenidae sp. 8 Setarches guentheri	4 1 26 2	21 10 8	2 12 9 1 2	27 23 35 2 1 2 8	24 21 8	2 2 35 2	1 1 1
Spariformes Lophiiformes	Callanthiidae	<i>Grammatonotus laysanus</i> Lophiiformes	1		13	13 1	13 1		
	Chaunacidae	Chaunax sp. Chaunax umbrinus	3 4	4	1	3 9		3 9	
	Lophiidae	Lophiidae Lophiodes cf. bruchius Lophiodes miacanthus	5	1 2 2	7	1 14 2	4		1 10 2
	Ogcocephalidae	Halieutaea retifera Malthopsis mitrigera* Solocisquama erythrina*	1 6		1 13 3	2 19 3	2 2 1	5	12 2

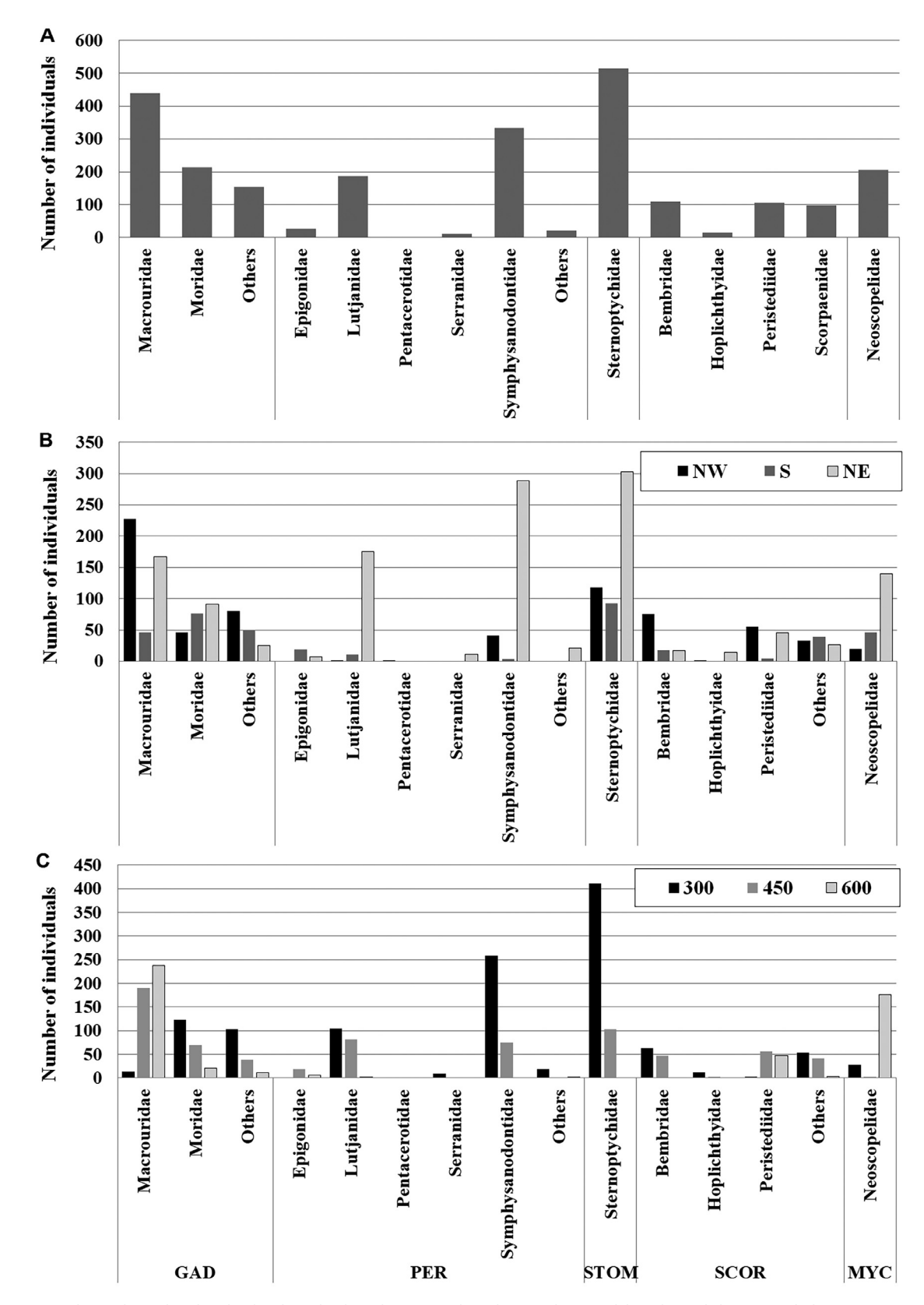


Fig. 2. Total number of individuals identified in the most abundant orders and families of deep-sea fishes on Pioneer Bank (A) overall, (B) by seamount side, and (C) by depth (m). GAD: Gadiformes; PER: Perciformes; STOM: Stomiiformes; SCOR: Scorpaeniformes; MYC: Myctophiformes

Table 4. Univariate permutational multivariate ANOVA (PERMANOVA) analysis of fish assemblages from Pioneer Bank based on a 2-way crossed model with 2 factors: sides and depth. Comparisons of each variable among sides and depths were made using Euclidean distance and 10 000 permutations; p-values ≤ 0.05 are in **bold**

Factors	Side $df = 2$		Depth $df = 2$		Side \times Depth df = 4		
	Pseudo- <i>F</i>	p	Pseudo-F	p	Pseudo-F	p	
Abundance (ind. / no. photos)	5.2554	0.016	0.3117	0.750	3.6855	0.024	
Species richness (S)	5.2725	0.015	0.2337	0.798	1.0881	0.404	
Estimated species richness (Es (300))	5.0915	0.020	0.2068	0.819	1.2098	0.350	
Shannon diversity (H')	5.0253	0.024	2.5649	0.107	1.7495	0.200	
Simpson dominance (D)	4.4976	0.029	2.9015	0.092	1.8450	0.172	

Table 5. Multivariate PERMANOVA and pairwise analyses of fish assemblage structure from Pioneer Bank, based on a 2-way crossed model with 2 factors: side and depth. Comparisons of each variable among sides and depths were based on the fourth root transformed relative abundance data (individuals / no. photos), Bray-Curtis similarity matrices, and $10\,000$ residual permutations. Monte Carlo (MC) tests were used for pairwise comparisons. For all tests, $p \le 0.05$ is indicated in **bold**. Coefficient of variation (CV) was used to determine the most important factor

Multivariate	PERMA	NOVA						
	df	Pseu	ıdo- <i>F</i>	p (perm)	Sqrt (CV)	CV%	
Side	2	3.5	696	<(0.001	20.182	17.0	
Depth	2	10.	10.456		0.001	38.862	32.7	
Side × Depth	4	2.1	763	<(0.001	23.607	19.9	
Residual	16				36.013	30.3		
Pairwise con	ıparisoı	ıs						
Depth			St	tudy	sites —			
interaction		NW		S	}	N	νE	
	t	p (MC)	t		p (MC)	t	p (MC)	
300, 450	2.9169	0.009	1.488	38	0.196	1.2812	0.217	
300, 600	4.08	0.003	1.761	19	0.076	2.2352	0.026	
450, 600	4.6942	0.002	1.817	73	0.076	2.4324	0.017	
Study site int	eractio	ns						
			—Depth	ı sa	mpled (r	n)		
		300		450		6	00	
	t	p (MC)	t		p (MC)	t	p (MC)	
NW, S	1.8176	0.075	2.210)2	0.046	1.9938	0.044	
NW, NE	1.4678	0.146	1.249	95	0.243	1.7059	0.074	
S, NE	1.3103	0.241	1.485	52	0.163	1.7861	0.055	

tests, these differences were at 450 m between the NW side and the other 2 sides due to the high relative abundance found on the NW side of the bank (Fig. S2 in Supplement 2). Species richness, $E_{S\,(300)}$, Shannon diversity, and Simpson dominance were significantly different among sides, but not among depths or their interaction (Table 4). The pairwise test for the species richness and $E_{S\,(300)}$ showed differences between the S side and the other 2 sides; for Shannon diversity between the S and NW sides; and Simpson dominance between the NW and the other 2 sides

(Fig. S2). The S side had the lowest diversity and highest dominance, whereas the NW side had the highest diversity and lowest dominance (Fig. S2).

3.3. Deep-sea fish assemblage structure

Significant variation in the fish assemblage structure for side and depth and their interaction was observed on Pioneer Bank (Table 5). The PERMANOVA model explained 69.6% of the variation, with depth as the most important factor (32.7%). The pairwise comparisons for the interaction showed that for a given side, there were differences between all depths in the NW, between either 300 or 450 m vs. 600 m on the NE side, but no differences with depth on the S side. Within a given depth, significant differences were observed between the NW and S sides at 450 and 600 m (Table 5).

The results obtained with the PERM-ANOVAs are visualized in the NMDS ordination (Fig. 3) and cluster dendrogram (Fig. S3 in Supplement 2), in which the data are clustered more by depth than by sides of the seamount. At 30% similarity, there is a clear separation

of 600 m depth transects from those at 300 and 450 m, but some overlap between 300 and 450 m, and of the three 300 m NE transects, 2 are grouped separately. Within the 600 m depth cluster, transects from a given side were more similar to each other than to the other sides. Among the 300 and 450 m transects, the 450 m NW and NE transects clustered with the 300 m NW transects and 1 transect from each of 300 m S and NE. The remainder of the 300 and 450 m transects fell outside this group (Fig. 3).

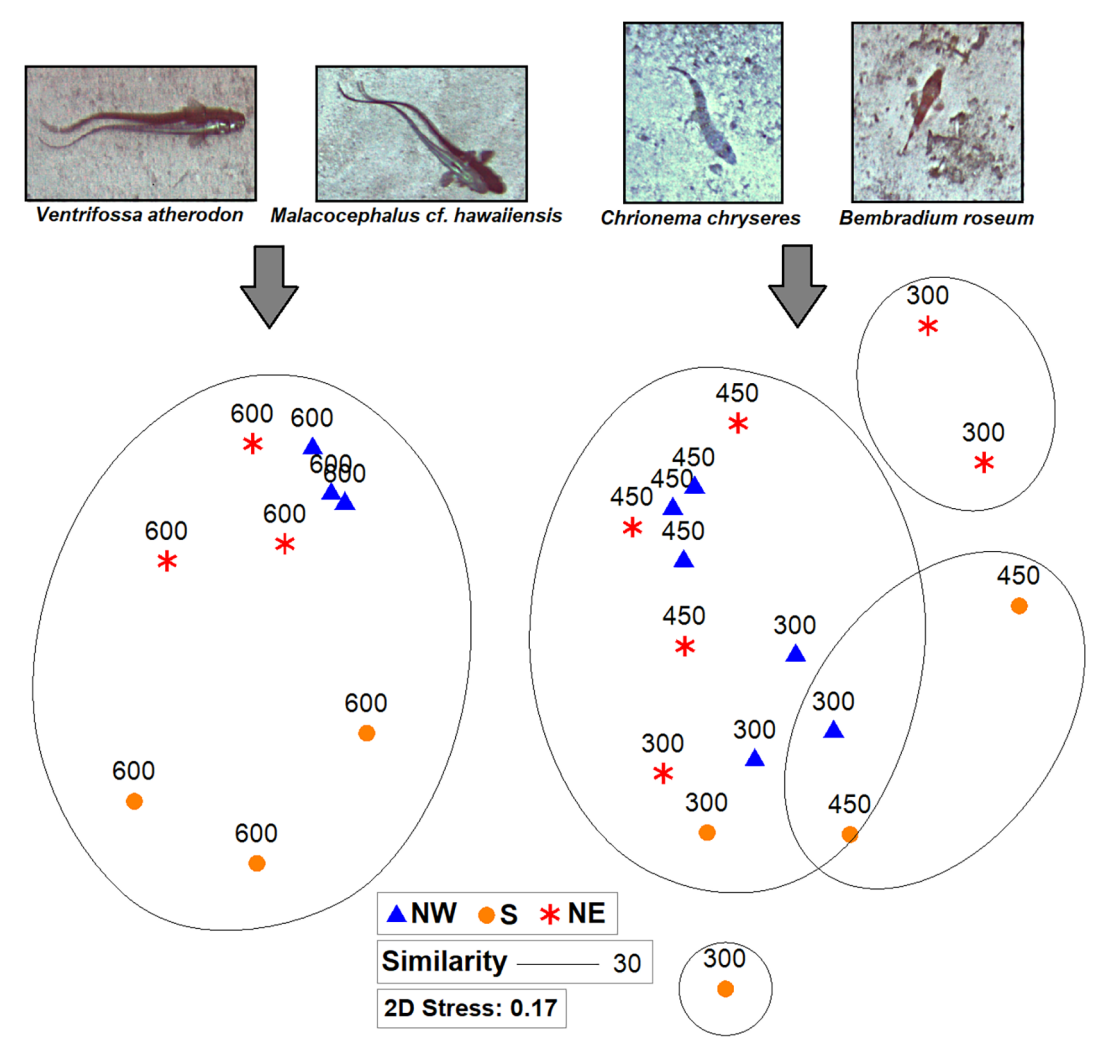


Fig. 3. Assemblage structure distribution by seamount side and depth in a non-metric multidimensional scaling (NMDS) ordination based on Bray-Curtis similarities calculated on the fourth root transformed relative abundance data. Each point represents a single transect. NW, S, and NE indicated with colored symbols represent sides on Pioneer Bank as in Table 2. Two main clusters are formed with 300–450 m depth and 600 m depth from which the most abundant species are shown

The SIMPER analysis showed that the most important species contributing to the dissimilarities on the NW side between 300 and 450 m were Coelorinchus gladius and Malacocephalus cf. hawaiiensis present only at 450 m; between 300 and 600 m, Chlorophthalmus providens and M. cf. hawaiiensis with presence only at 600 m; and between 450 and 600 m, Argyripnus sp. and Symphysanodon maunaloae present only at 450 m (Table 3; Table S3 in Supplement 1). Dissimilarities on the NE side between 300 and 600 m were mostly due to Symphurus strictus present only at 600 m, and Symphysanodon maunaloae present only at 300 m. Between 450 and 600 m, Symphurus strictus and Neoscopelus macrolepidotus present only at 600 m were responsible for most of the dissimilarities between the depths. Differences

between the NW and S, among the 450 m depth transects, were mostly due to the presence of *Argyripnus* sp. and *M.* cf. *hawaiiensis* only on the NW side of the Bank, while among 600 m depths, differences were mostly due to *C. proridens* and *Scalicus hians* present also only on the NW side (Table S3).

Based on SIMPER similarity, the cluster with depths of 300 and 450 m showed the lowest average similarity (34.02%) and was characterized by *Chrionema chryseres* (19.75%) and *Bembradium roseum* (15.32%) with contributions higher than 10%. The cluster with the 600 m transects had an average similarity of 43.34% and was represented by *M.* cf. *hawaiiensis* and *Ventrifossa atherodon* with a contribution of 15.85 and 10.16%, respectively (Table S3).

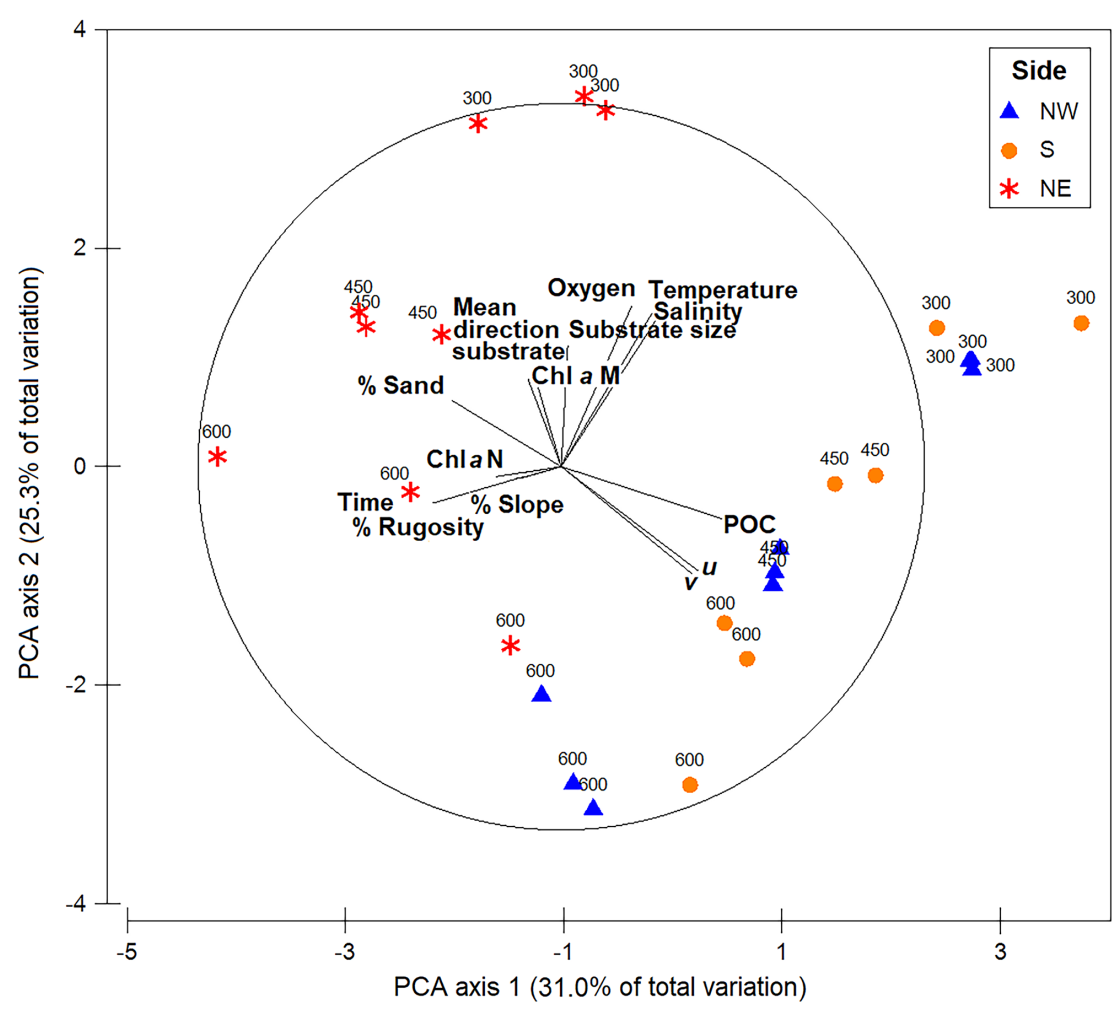


Fig. 4. Principal component analysis (PCA) of the environmental variables by transect at 300, 450, and 600 m on Pioneer Bank. The first 2 axes of the PCA accounted for 56.3 % of the total variance. Vectors show the direction and strength of each environmental variable relative to the overall distribution. Sides on Pioneer Bank (NW, S, and NE) are indicated with colored symbols, and depth values are shown for each transect

3.4. Habitat description

The NW side of Pioneer Bank showed lower average values of dissolved oxygen and higher average temperature compared to the other 2 sides. Salinity was very similar on the 3 sides (Table S1). Mean direction of the substrate (as defined in Section 2.3) was very different among the 3 sides. Sandy substrates with pebbles and high percentages of low rugosity predominated on the NE side, while hard substrates predominated on the NW and S sides. The NW side had mostly intermediate percentages of low rugosity with cobble, and the S side had very low smooth rugosity with coral rubble substrates. The S side had the highest average POC with the lowest average POC with the highest average chl a. The NW side had the highest average chl a. The NW side had the highest

est average current vector v (north-south) and the lowest average current vector *u* (east–west), while the NE side had the lowest average current factor v and the highest average current factor u (Table S1). Dissolved oxygen, temperature, and salinity decreased with depth on each side, but most of the substrate variables did not show a clear pattern based on depth on each side (Table S1). A PCA plot of environmental data for each transect shows a clear separation of the NE side from the other 2 sides as well as a gradient of depth diagonally across the plot. The 300 m NE side transects, and 600 m NW and S transects separate from the other transects on all 3 sides along PCA axis 2, which was most strongly correlated with oxygen, temperature, and salinity (Fig. 4; Table S4 in Supplement 1). Along PCA axis 1, the 300 m NW and S transects separate from the transects on the other sides

Table 6. Distance-based linear model (DistLM) marginal test results and model selection based on the environmental variables used to evaluate correlation with the deep-sea fish community structure patterns on Pioneer Bank; $p \le 0.05$ is indicated in **bold**

Variable no.	Variable	SS(trace)	Pseudo-F	p	Proportion of variation	
1	Salinity	14530	6.1048	0.0002	0.2098	
2	Mean direction substrate	e 5315.4	1.9116	0.054	0.0767	
3	% slope	3759.1	1.3197	0.175	0.0543	
4	% rugosity	7847.2	2.9384	0.008	0.1133	
5	Grain size	4509.5	1.6015	0.110	0.0651	
6	Chl a (NESDIS)	6828	2.5150	0.018	0.0986	
7	V	2942	1.0201	0.394	0.0424	
8	Time of day	4590.6	1.6324	0.102	0.0663	
Overall b	est solutions					
No. of variables	AIC	\mathbb{R}^2	RSS		Selections	
4		4506	38055		1,2,4,6	
5		0.4906 35287			1,2,4,6,7	
5		4849	35680		1,2,4,6,8	
6		5232	33030		1,2,4,6-8	
4		4383	38909		1,2,6,7	
5		0.4797 3			1-4,6	
6		5195	33282	_	1-4, 6, 7	
7		5544	30867		1-4,6-8	
6		5164	33502		1-4,6,8	
5	194.10 0.	4743	36418	3	1, 2, 4-6	

(Fig. 4). This axis was correlated with POC and current factors u and v (Fig. 4; Table S4).

3.5. Habitat effects

The DistLM marginal tests showed that salinity,% rugosity, and chl a (extracted from NESDIS) explained a significant amount of the variation (p < 0.05, Table 6); with proportions from 21 to 10% (Table 6). The top 10 models from the DistLM had AIC values with a range of only 0.9 and included 4–7 variables. Although mean direction of the substrate did not explain a significant amount of variation (p = 0.054) as an individual variable (Table 6), the best model included this variable along with salinity, % rugosity, and chl a. Nine of the top 10 models included these 4 variables. The first 2 axes of the fitted model ordination (dbRDA, Fig. 5) explained 80.3% of the fitted variation of the structure of the deep-sea fish assemblages on Pioneer Bank with salinity highly and positively correlated with the first axis and possibly explaining the differences between depths. Chl a was highly and negatively correlated with the second dbRDA axis and potentially explains the differences between the S and the other 2 sides (Fig. 5).

There were no clear patterns in the bubble plots to corroborate the correlation between assemblage structure and the environmental variables recognized as important by DistLM, except for salinity (Fig. S4 in Supplement 2). Deeper depths showed lower salinity and shallower depths higher salinity (Fig. S4A). Percentage rugosity, chl *a*, and mean direction of substrate did not show a noticeable pattern by depth, nor with a particular direction in the ordination.

4. DISCUSSION

Since quantitative analyses have recently indicated significant spatial variation of fishes within a single seamount in the PMNM (Mejía-Mercado et al. 2019), it is important to document these variations across multiple locations to determine if there are generalizable patterns within the greater

NWHI region or for seamounts in general. Including environmental data in studies may reveal a common factor contributing to the observed patterns. Fish assemblages on Necker Island in the NWHI varied in structure by side, depth, and the interaction of both factors; based on the best DistLM model, this variation was most correlated with dissolved oxygen (and its correlate temperature), salinity, percentage of sand (and its correlate substrate size), rugosity, slope, POC (and its correlate chl a), and current vectors u and v (Mejía-Mercado et al. 2019). The present study generated information on the variation in the deepsea fish fauna inhabiting a second seamount protected in the PMNM. As expected, based on observations on Necker, the fish assemblage structure on Pioneer Bank varied horizontally, with differences between the sides of the seamount, and vertically, with differences between the 3 depths with similar environmental variables driving these differences.

4.1. Species richness and composition of the fish assemblage

The deep-sea fish assemblages on Pioneer Bank were characterized by a high abundance of the

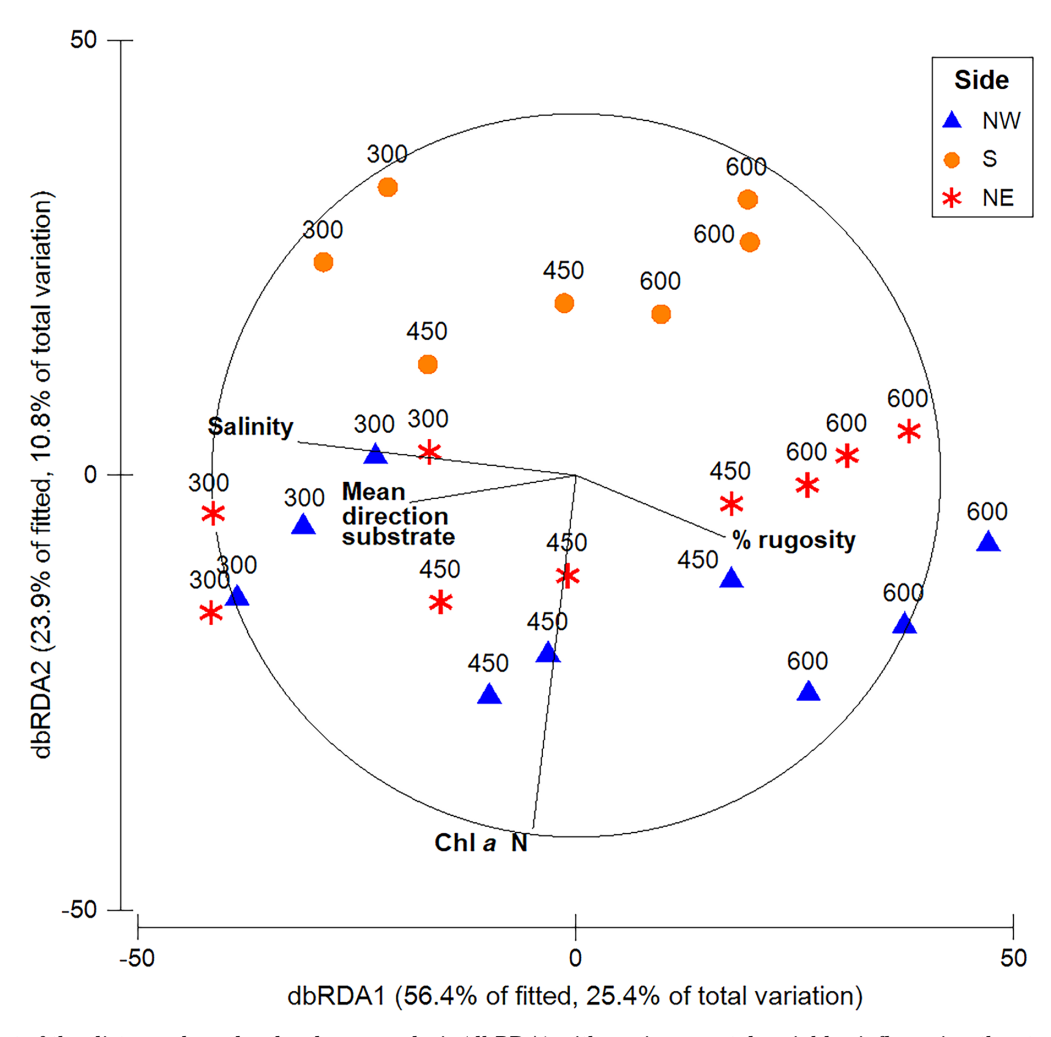


Fig. 5. Biplot of the distance-based redundancy analysis (dbRDA) with environmental variables influencing the structure of the deep-sea fish assemblage on Pioneer Bank. The environmental covariates were superimposed onto the dbRDA plot as vectors whose direction and length are related to their partial correlation with the dbRDA axes. Sides on Pioneer Bank are indicated with colored symbols, and depth values are shown for each transect

families Sternoptychidae, Symphysanodontidae, and Macrouridae, with the highest abundance of the first 2 families on the NE side of the bank at 300 m and for the third family on the NW side at 600 m (Fig. 2). These deep-sea fish assemblages on Pioneer Bank generally were similar to those on Necker Island (Mejía-Mercado et al. 2019) except for the family Symphysanodontidae represented by Symphysanodon maunaloae (Table 3). S. maunaloae has been observed on some seamounts in the Hawaiian Archipelago and at Johnston Atoll swimming near the bottom over different types of substrates at depths from 130 to 400 m (Chave & Mundy 1994, Chave & Malahoff 1998). On Necker Island, this species was found in areas with sandy and hard substrates (Mejía-Mercado et al. 2019), while on Pioneer Bank, it was highly abundant on the NE side on transects that

were characterized by sandy substrates with pebbles (Table S1). Therefore, a preference for a specific type of substrate does not seem to explain the higher abundance of this species on Pioneer Bank. Interannual variability due to differences in the years sampled could affect the differences in the abundance of this species within Pioneer, but not between Pioneer and Necker, as both Necker and the NE of Pioneer were sampled during 2015. On the other hand, topdown effects may be influencing differences in the abundance of this species between the 2 seamounts. Seki & Callahan (1988) reported that S. maunaloae is one of the species that are mostly consumed by the lutjanid Pristipomoides zonatus in the Mariana Archipelago. A congeneric species of lutjanid was identified in our study, the opakapaka or pink snapper P. filamentosus, which has been observed feeding primarily on plankton, but with some feeding on fish as well (Haight et al. 1993). If there were a similar trophic relationship between *P. filamentosus* and *S. maunaloae*, it could explain the differences in the abundance of *S. maunaloae* between the 2 seamounts, as *P. filamentosus* was observed with low abundance and *S. maunaloae* with very high abundance on Pioneer Bank, with the opposite observed on Necker (Mejía-Mercado et al. 2019). Thus, the differences between the 2 seamounts in the abundance of *S. maunaloae* may be attributable to predation effects.

Of the 66 species identified with a full scientific name on Pioneer Bank, 38 had been previously described in the larger Hawaiian Archipelago, including Pioneer Bank (Mundy 2005, Daly-Engel et al. 2018). However, the other 28 species had been observed at smaller areas that did not include Pioneer Bank. That is, 18 were thought to only inhabit the Main Hawaiian Islands (MHI) (Mundy 2005), 5 were known from the MHI and the NWHI to the southeast of Pioneer Bank (Mundy 2005), 3 were recently reported on Necker Island (Mejía-Mercado et al. 2019), and 2 were reported on seamounts in the NWHI at sites to the northwest of Pioneer Bank (Mundy 2005).

As demonstrated by these results, studying the fauna that inhabits a seamount can provide valuable information about fish distribution on other seamounts that are part of the same chain, as well as help to understand possible connectivity between these seamounts. For example, of the 81 species identified at 300, 450, and 600 m on Pioneer Bank, 75 species were also observed by Mejía-Mercado et al. (2019) on Necker Island in the same depth range. The remaining 6 were rare species on Pioneer Bank (e.g. Pseudotriakis microdon, Pristilepis oligolepis, and Bodianus sanguineus, Table 3). With almost 920 km of separation between these 2 seamounts and no other non-seamount seafloor within this depth range, it is likely that seamounts in the PMNM are acting as dispersal stepping stones for deep-sea fish species as was first proposed by Hamilton (1956) and discussed in detail by Wilson & Kaufman (1987). Although genetic studies should be conducted to corroborate this assumption, evidence in benthopelagic fishes has demonstrated that some populations are not different among seamounts that are separated by hundreds, or even thousands of kilometers (e.g. Aboim 2005).

Having more extensive lists of species and their specific ranges increases the opportunity to improve the management and conservation of the region (Kennedy et al. 2019). For example, some of the ob-

served species on Pioneer Bank are fisheries targets outside the PMNM (Uchida & Uchiyama 1986, Morato et al. 2006), including the alfonsinos *Beryx decadactylus* and *B. splendens*, and the pelagic armourhead *Pentaceros wheeleri* (Table 3). These species, which are seamount-aggregating, are considered vulnerable due to the limited habitat for them on individual seamounts (compared to continental areas) and their sporadic recruitment (Lehodey et al. 1997, Kiyota et al. 2016). The occurrence of these species on this protected seamount may be important information for management, as they are actively fished on seamounts outside the US exclusive economic zone.

4.2. Fish assemblage patterns

Differences in the relative abundance of fish were more related to conditions at specific locations than to depth. Differences in the abundance of megafauna have previously been attributed to changes in depth, with a decrease in abundance observed with increasing depth (Rex & Etter 2010). Nevertheless, similar to what was observed on Necker Island (Mejía-Mercado et al. 2019), differences in fish abundance on Pioneer Bank are more closely related to specific characteristics of a given geographic location (side) of the seamount. Some studies have found that the topography of the seamount and currents together may determine the amount of food that reaches different depths from the surface (Rogers 1994, White et al. 2007). In addition, the type and complexity of the substrate found on a given side of the seamount and, within either side, at a given depth, can determine the amount of organic matter that is retained and available for consumption (Boehlert & Genin 1987). In this study, although the NW side of the seamount at 450 m showed no differences in the mean values for current vectors, POC, and chl a among the 3 sides (Table S1), differences in the characteristics of the substrate were noted. That is, the intermediate rugosity with cobblestones and some percentage of sand observed at 450 m on the NW side of Pioneer Bank may offer more suitable conditions to allow the fish species inhabiting this area to increase their abundance. Although it has been observed that the high complexity of the seafloor is associated with a high abundance of fish (Leitner et al. 2021), differences in trophic preferences and life-history traits could influence the relationship between fish abundance and habitat complexity (see Ferrari et al. 2018).

Diversity metrics also varied by side of the bank, possibly driven by differences in substrate complexity and the current regime. The variation by side rather than by depth observed in this study contrasts with the findings on Necker Island, where all diversity metrics were significantly different by the depth and the interaction of side and depth (Mejía-Mercado et al. 2019). Variations in fish species richness by depth are a common pattern in the general deep sea (Rex 1981), with a peak at bathyal depths around 400-600 m (Froese & Sampang 2004, Mejía-Mercado et al. 2019) and influenced by water masses (Koslow et al. 1994, Clark et al. 2010a, Tracey et al. 2012, Mejía-Mercado et al. 2019). Depths were chosen in this study based on the fish assemblage changeover observed on Necker Island (Mejía-Mercado et al. 2019), which could have attenuated possible differences by depth in these metrics on Pioneer Bank. These results suggest that depth patterns may vary among seamounts, and a higher-resolution survey may be required for each seamount to capture the full range of variability for that seamount. Variation in fish species richness has also been associated with different substrate characteristics and their interaction with the hydrodynamic components, such as currents (Borland et al. 2021). High rugosity has been related to high species richness or diversity in seamounts (Oyafuso et al. 2017). However, the S side of Pioneer Bank, with the highest rugosity among sides, showed the lowest species richness and diversity, and the highest dominance (Table S1). Another possibility is that currents and their association with substrates showing high rugosity could be playing an important role on this side (Borland et al. 2021). However, surface currents had an intermediate value relative to the other 2 sides (Table S1). Deeper currents that were not measured in this study may instead be influencing the low diversity of species estimated on this side.

The community structure of the fish assemblage had significant differences by side, depth, and side-by-depth interactions (Table 5). Variations in deep-sea fish assemblages on seamounts have been previously observed, both vertically and horizontally (Tracey et al. 2004, McClain et al. 2010, Mejía-Mercado et al. 2019); however, vertical variations seem to have a greater influence on fish assemblage patterns than horizontal variations. According to the coefficient of variation, depth was the most important factor in explaining the PERMANOVA results (Table 5) for the fish assemblage on Pioneer Bank. This result was also supported by the NMDS plot and the cluster dendrogram, which showed a better separa-

tion of transects by depth than by sides. Similar results were observed on Necker Island, in which the variation of the assemblage structure was more evident by depth with a horseshoe effect in the NMDS plot (Mejía-Mercado et al. 2019). In the current study, the transects at depths of 300 and 450 m overlapped, but there was a clear separation of 600 m depth transects (Fig. 3). The fish assemblage at 300 and 450 m was characterized by the duckbill Chrionema chryseres and the scorpionfish Bembradium roseum (Table S3), which were not observed as important species in their contributions to the assemblages at similar depths on Necker Island (Mejía-Mercado et al. 2019). However, at 600 m, where the assemblage was represented by the macrourids Malacocephalus cf. hawaiiensis and Ventrifossa atherodon, the same species that were also important in the assemblage on Necker Island from 550 to 700 m (Mejía-Mercado et al. 2019).

These differences among seamounts indicate the need to conduct more ecological studies at different depths on this seamount and other seamounts in the PMNM to elucidate the full range of variation. This information is crucial to better understand the extent of the variation of deep-sea fishes in the archipelago and to fill gaps in management and conservation strategies.

4.3. Environmental variables driving fish assemblage structure

Fish assemblage structure on Pioneer Bank was most strongly correlated with salinity, % rugosity, chl a, and mean direction of substrate (Table 6, Fig. 5). Salinity explained the highest proportion of the variation of any individual environmental variable. Salinity is generally not an influential variable in the ecology of deep-sea organisms (Thistle 2003) but rather is related to water masses. More likely one or both of the strong correlates of salinity; temperature and oxygen (Table S2) were the influential variables. Temperature is known to affect the physiology of organisms (Thistle 2003, Clark et al. 2010b) and is therefore likely to influence their distribution on the bank. Similarly, oxygen is known to be a strong correlate of species distributions in the deep sea (e.g. Yeh & Drazen 2009, Mejía-Mercado et al. 2019).

Rugosity is an important component and indicator of complexity in soft or hard benthic habitats (Wilson et al. 2007, Stamoulis et al. 2018). Changes in rugosity have been associated with variations in fish

abundance and diversity (e.g. Kelley et al. 2006, Oyafuso et al. 2017). Areas with high rugosity increase the probability of food retention, making it available to more organisms that will eventually increase in number, but they also offer a diversity of niches for more species to settle and remain in these areas (Ferrari et al. 2018). However, some cases can be outside of these generalities when it comes to habitat preferences for feeding, shelter, reproduction, or simply life history. Our results show that the 2 benthic species C. chryseres and B. roseum that characterized the 300-450 m assemblage (Table S3) were very abundant on substrates with high rugosity (low % of smooth surface) on the NW and S sides (Table S1). In contrast, the demersal species M. cf. hawaiiensis and V. atherodon (Table S3), which represented the 600 m assemblage, were observed with high abundance on substrates with low rugosity (high % of smooth surface) on the NW and NE sides of the bank (Table S1). These 2 demersal species were also observed on Necker Island with high abundance at 600 m, but in substrates with high rugosity (Mejía-Mercado et al. 2019). These differences in rugosity preferences for the same species suggest that rugosity might not be as important of a driver of community structure for more demersal species. Benthic species are in physical contact with the bottom but are not very mobile, whereas demersal species spend most of their lives near the bottom but are actively moving (Randall & Farrell 1997), which allows them to inhabit substrates with different rugosity that offer more prey options, for example.

Chl a was also an important variable explaining the variation in fish assemblage structure. The observed increase in chl a over seamounts (Genin & Boehlert 1985, Dower et al. 1992, Mouriño et al. 2001) has been controversial, but a recent study focused on several seamounts in the Pacific Ocean confirmed that chl a concentrations increased by up to 56% compared to surrounding oceanic conditions (Leitner et al. 2020). As the spatial variability of chl aconcentrations from one seamount to another can be affected by advection over a seamount and stratification of the water column (White et al. 2007), likely, each side of the seamount may also show differences in chl a levels. Our results showed that the average surface chl a concentrations were higher on the NW side and lower on the S side (Table S1). These distinct values of chl a may be influencing the differences observed in the fish assemblage structure between the NW and S sides at 450 and 600 m (Table 5). This can be supported by the results obtained by Mejía-Mercado et al. (2019), where POC and its correlate chl *a* were important variables explaining the variation in fish assemblage on Necker Island.

Mean direction of the substrate did not itself explain a significant amount of the variation in the assemblage structure, but it was an important variable in the overall model from DistLM. Aspect as a topographic feature indicates the direction the slope is facing, and could determine the distribution of some fishes, because the orientation of the slope relative to currents may have a big influence on localized currents over specific areas of a seamount. At 450 and 600 m, where differences in the fish assemblage structure were observed between the NW and S sides, the averages of mean direction of substrate values were very different (Table S1). However, we cannot go any further in explaining the influence of this variable in the assemblage structure because deep currents were not measured in this study. Therefore, more studies that include the association between topographic characteristics and deep currents would be necessary to better understand how aspect may be directly or indirectly affecting the structure of fish assemblages.

5. CONCLUSIONS

Variation in fish abundance and assemblage structure on Pioneer Bank, with both study site and depth, and variations in species richness, dominance, and diversity by side, support the evidence of significant community variation within a single seamount. These scales of spatial variability both with depth and across short horizontal distances observed on Pioneer Bank are similar to those found on the nearby seamount, Necker Island, and other seamounts. At least 2 assemblages of fishes were observed, one between 300 and 450 m, and another at 600 m. The variability of the assemblage structure was correlated with salinity, % rugosity, chl a, and mean direction of the substrate. This study constitutes the first detailed contribution to the knowledge of the deep-sea fish fauna present on Pioneer Bank. It can be considered as an ecological baseline for the management and conservation of seamounts in the PMNM and other areas. More studies should be conducted in the area to continue filling in gaps in the patterns of species distributions, abundance, and species composition of deep-sea fish that can inform the management of seamounts and the PMNM.

Acknowledgements. This study was conducted through NSF grants OCE-1334652 to A.R.B. and OCE-1334675 to E. Brendan Roark. Work in the PMNM was carried out under permit #PMNM-2014-028. B.E.M.M. was supported by a fellowship from Colciencias-Fulbright. We thank Bruce Mundy for helping in the identification of the fish species as well as helping with the revision of the manuscript. We also thank the crews of the AUV 'Sentry,' the RV 'Sikuliaq,' and RV 'Kilo Moana.' Nicole Morgan partitioned the AUV dives into transects and compiled the environmental data by transect. Mauricio Silva extracted from databases surface chl a, POC, and current vectors by transect.

LITERATURE CITED

- Aboim MA (2005) Population genetics and evolutionary history of some deep-sea demersal fishes from the Azores-North Atlantic. PhD dissertation, University of Southampton
- Akaike H (1973) Information theory as an extension of the maximum likelihood principle. In: Petrov BN, Csaki F (eds) Second International Symposium on Information Theory. Akademiai Kiado, Budapest, p 267–281
- Anderson MJ, Gorely RN, Clarke KR (2008) PERM-ANOVA+Primer: guide to software and statistical methods. Primer-E, Plymouth
- Baco AR, Morgan N, Roark EB, Silva M, Shamberger KE, Miller K (2017) Defying dissolution: discovery of deep-sea scleractinian coral reefs in the North Pacific. Sci Rep 7:5436
- Baco AR, Roark EB, Morgan NB (2019) Amid fields of rubble, scars, and lost gear, signs of recovery observed on seamounts on 30- to 40-year time scales. Sci Adv 5:eaaw4513
- *Baco AR, Morgan NB, Roark EB (2020) Observations of vulnerable marine ecosystems and significant adverse impacts on high seas seamounts of the Northwestern Hawaiian Islands and Emperor Seamount Chain. Mar Policy 115:103834
 - Beyer HL (2012) Geospatial modelling environment (Version 0.7.2.0) (software). https://pdf4pro.com/cdn/geospatial-modelling-environment-spatial-156afa.pdf
- Blair TC, McPherson JG (1999) Grain-size and textural classification of coarse sedimentary particles. J Sediment Res 69:6–19
- Bo M, Bertolino M, Borghini M, Castellano M and others (2011) Characteristics of the mesophotic megabenthic assemblages of the Vercelli seamount (North Tyrrhenian Sea). PLOS ONE 6:e16357
 - Boehlert GW, Genin A (1987) A review of the effects of seamounts on biological processes. In: Keating BH, Fryer P, Batiza R, Boehlert GW (eds) Seamounts, islands, and atolls. Geophys Monogr Ser 43. American Geophysical Union, Washington, DC, p 319–334
- Borland HP, Gilby BL, Henderson CJ, Leon JX and others (2021) The influence of seafloor terrain on fish and fisheries: a global synthesis. Fish Fish 22:707–734
 - Carpenter KE, Niem VH (eds) (1998) FAO species identification guide for fishery purposes. The living marine resources of the western central Pacific. Cephalopods, crustaceans, holothurians and sharks, Vol 2. FAO, Rome
 - Carpenter KE, Niem VH (eds) (1999a) FAO species identification guide for fishery purposes. The living marine resources of the western central Pacific. Batoid fishes, chimaeras and bony fishes part 1 (Elopidae to Lino-

- phrynidae), Vol 3. FAO, Rome
- Carpenter KE, Niem VH (eds) (1999b) FAO species identification guide for fishery purposes. The living marine resources of the western central Pacific. Bony fishes part 2 (Mugilidae to Carangidae), Vol 3. FAO, Rome
- Carpenter KE, Niem VH (eds) (2001a) FAO species identification guide for fishery purposes. The living marine resources of the western central Pacific. Bony fishes part 3 (Menidae to Pomacentridae), Vol 3. FAO, Rome
- Carpenter KE, Niem VH (eds) (2001b) FAO species identification guide for fishery purposes. The living marine resources of the western central Pacific. Bony fishes part 4 (Labridae to Latimeriidae), estuarine crocodiles, sea turtles, sea snakes, and marine mammals, Vol 3. FAO, Rome
- Chatterjee S, Hadi AS, Price B (2000) Regression analysis by example. John Wiley and Sons, New York, NY
- Chave EH, Malahoff A (1998) In deeper waters: photographic studies of Hawaiian deep-sea habitats and lifeforms. University of Hawaii Press, Honolulu, HI
- Chave EH, Mundy BC (1994) Deep-sea benthic fish of the Hawaiian Archipelago, Cross Seamount, and Johnston Atoll. Pac Sci 48:367–409
- Clark MR, Althaus F, Williams A, Niklitschek E and others (2010a) Are deep-sea fish assemblages globally homogenous? Insights from seamounts. Mar Ecol 31(Suppl 1): 39–51
- Clark MR, Rowden AA, Schlacher T, Williams A and others (2010b) The ecology of seamounts: structure, function, and human impacts. Annu Rev Mar Sci 2:253–278
- Clark MR, Schlacher TA, Rowden AA, Stocks KI, Consalvey M (2012) Science priorities for seamounts: research links to conservation and management. PLOS ONE 7:e29232
 - Clarke KR, Warwick RM (2001) Change in marine communities: an approach to statistical analysis and interpretation, 2nd edn. Primer-E, Plymouth
- Daly-Engel TS, Koch A, Anderson JM, Cotton CF (2018)
 Description of a new deep-water dogfish shark from
 Hawaii, with comments on the Squalus mitsukurii species
 complex in the West Pacific. ZooKeys 798:135–157
- Devine BM, Baker KD, Edinger EN, Fisher JA (2020) Habitat associations and assemblage structure of demersal deepsea fishes on the eastern Flemish Cap and Orphan Seamount. Deep Sea Res I 157:103210
- Nower J, Freeland H, Juniper K (1992) A strong biological response to oceanic flow past Cobb Seamount. Deep Sea Res I 39:1139–1145
 - Esri (Environmental System Research Institute, Inc.) (2016) ArcGIS Desktop: Release 10.4.1. Environmental Systems Research Institute, Redlands, CA
- Ferrari R, Malcolm HA, Byrne M, Friedman A and others (2018) Habitat structural complexity metrics improve predictions of fish abundance and distribution. Ecography 41:1077–1091
 - Fisher NI (1995) Statistical analysis of circular data. Cambridge University Press, Cambridge
 - Fofonoff NP, Millard RC Jr (1983) Algorithms for computation of fundamental properties of seawater. Endorsed by UNESCO/SCOR/ICES/IAPSO Joint Panel on Oceanographic Tables and Standards and SCOR Working Group 51. UNESCO Tech Pap Mar Sci 44:1–54
 - Froese R, Sampang A (2004) Taxonomy and biology of seamount fishes. In: Morato T, Pauly D (eds) Seamounts: biodiversity and fisheries. Fisheries Centre Research Reports, Vol 12, no. 5. Fisheries Centre, University of British Columbia, Vancouver, p 25–32

- Genin A (2004) Bio-physical coupling in the formation of zooplankton and fish aggregations over abrupt topographies. J Mar Syst 50:3–20
- Genin A, Boehlert GW (1985) Dynamics of temperature and chlorophyll structures above a seamount: an oceanic experiment. J Mar Res 43:907–924
 - Haight WR, Kobayashi DR, Kawamoto KE (1993) Biology and management of deepwater snappers of the Hawaiian archipelago. Mar Fish Rev 55:17–24
 - Hamilton EL (1956) Sunken islands of the mid-Pacific mountains. Geological Memoirs, Vol 64. Geological Society of America. New York, NY
- Husebo A, Nottestad L, Fossa JH, Furevik DM, Jorgensen SB (2002) Distribution and abundance of fish in deep-sea coral habitats. Hydrobiologia 471:91–99
 - Kelley CH, Moffitt RB, Smith JR (2006) Mega-to micro-scale classification and description of bottomfish essential fish habitat on four banks in the Northwestern Hawaiian Islands. Atoll Res Bull 543:319–332
- Kennedy BRC, Cantwell K, Malik M, Kelley C and others (2019) The unknown and the unexplored: insights into the Pacific deep-sea following NOAA CAPSTONE expeditions. Front Mar Sci 6:480
- Kikiloi K, Friedlander AM, Wilhelm A, Lewis N, Quiocho K, 'Āila W Jr, Kaho'ohalahala S (2017) Papahānaumo-kuākea: integrating culture in the design and management of one of the world's largest marine protected areas. Coast Manag 45:436–451
- Kiyota M, Nishida K, Murakami C, Yonezaki S (2016) History, biology, and conservation of Pacific endemics. 2. The North Pacific armorhead, *Pentaceros wheeleri* (Hardy, 1983) (Perciformes, Pentacerotidae). Pac Sci 70:1–20
- Koslow JA, Bulman CM, Lyle JM (1994) The mid-slope demersal fish community off southeastern Australia. Deep Sea Res I 41:113–141
- Lehodey P, Grandperrin R, Marchal P (1997) Reproductive biology and ecology of a deep-demersal fish, alfonsino *Beryx splendens*, over the seamounts off New Caledonia. Mar Biol 128:17–27
- Leitner AB, Neuheimer AB, Drazen JC (2020) Evidence for long-term seamount-induced chlorophyll enhancements. Sci Rep 10:12729
- Leitner AB, Friedrich T, Kelley CD, Travis S, Partridge D, Powell B, Drazen JC (2021) Biogeophysical influence of large-scale bathymetric habitat types on mesophotic and upper bathyal demersal fish assemblages: a Hawaiian case study. Mar Ecol Prog Ser 659:219–236
- Long DJ, Baco AR (2014) Rapid change with depth in megabenthic structure-forming communities of the Makapu'u deep-sea coral bed. Deep Sea Res II 99:158–168
- McClain CR (2007) Seamounts: identity crisis or split personality? J Biogeogr 34:2001–2008
- McClain C, Lundsten L, Barry J, DeVogelaere A (2010) Assemblage structure, but not diversity or density, change with depth on a northeast Pacific seamount. Mar Ecol 31:14–25
- Mejía-Mercado BE, Mundy B, Baco AR (2019) Variation in the structure of the deep-sea fish assemblages on Necker Island, Northwestern Hawaiian Islands. Deep Sea Res I 152:103086
- Milligan RJ, Spence G, Roberts JM, Bailey DM (2016) Fish communities associated with cold-water corals vary with depth and substratum type. Deep Sea Res I 114:43–54
 - Morato T, Clark MR (2007) Seamount fishes: ecology and life histories. In: Pitcher TJ, Morato T, Hart PJB, Clark

- MR, Haggan N, Santos RS (eds) Seamounts: ecology, fisheries, and conservation. Fish and Aquatic Resource Series 12. Blackwell, Oxford, p 170–188
- Morato T, Cheung WWL, Pitcher TJ (2006) Vulnerability of seamount fish to fishing: fuzzy analysis of life history attributes. J Fish Biol 68:209–221
- Morgan NB, Cairns S, Reiswig H, Baco AR (2015) Benthic megafaunal community structure of cobalt-rich manganese crusts on Necker Ridge. Deep Sea Res I 104:92–105
- Mortensen PB, Buhl-Mortensen L (2004) Distribution of deep-water gorgonian corals in relation to benthic habitat features in the Northeast Channel (Atlantic Canada). Mar Biol 144:1223–1238
- Mouriño B, Fernandez E, Serret P, Harbour D, Sinha B, Pingree R (2001) Variability and seasonality of physical and biological fields at the Great Meteor Tablemount (subtropical NE Atlantic). Oceanol Acta 24:167–185
 - Mundy BC (2005) Checklist of the fishes of the Hawaiian Archipelago. Bishop Mus Bull Zool 6:1–704
 - Nelson JS, Grande TC, Wilson MV (2016) Fishes of the world, 5th edn. John Wiley & Sons, Hoboken, NJ
 - NOAA (2019) Pioneer Bank: Bathymetry. www.soest.hawaii. edu/pibhmc/cms/data-by-location/northwest-hawaiianislands/submerged-banks/pioneer-bank/pioneer-bankbathymetry/
 - NOAA Office of National Marine Sanctuaries (2020) 2020 State of Papahānaumokuākea Marine National Monument: status and trends 2008–2019. US Department of Commerce, National Oceanic and Atmospheric Administration, Office of National Marine Sanctuaries, Silver Spring, MD
 - Oksanen J, Blanchet FG, Kindt R, Legendre P and others (2010) Vegan: community ecology package. R package version 1.17-4. https://cran.r-project.org/web/packages/vegan/index.html
- Oyafuso ZS, Drazen JC, Moore CH, Franklin EC (2017) Habitat-based species distribution modelling of the Hawaiian deepwater snapper–grouper complex. Fish Res 195:19–27
- Parrish FA, Boland RC (2004) Habitat and reef-fish assemblages of banks in the Northwestern Hawaiian Islands. Mar Biol 144:1065–1073
 - Randall JE (2007) Reef and shore fishes of the Hawaiian Islands. Sea Grant College Program, University of Hawai'i, Honolulu, HI
 - Randall DJ, Farrell AP (1997) Deep-sea fishes. Academic Press, San Diego, CA
- Rex M (1981) Community structure in the deep-sea benthos. Annu Rev Ecol Syst 12:331–353
 - Rex MA, Etter RJ (2010) Deep-sea biodiversity: pattern and scale. Harvard University Press, London
 - Rogers AD (1994) The biology of seamounts. Adv Mar Biol 30:305–350
- Rowden AA, Dower JF, Schlacher TA, Consalvey M, Clark MR (2010) Paradigms in seamount ecology: fact, fiction and future. Mar Ecol 31(Suppl 1):226–241
- Samadi S, Bottan L, Macpherson E, Richer De Forges B, Boisselier MC (2006) Seamount endemism questioned by the geographic distribution and population genetic structure of marine invertebrates. Mar Biol 149:1463–1475
 - Samadi S, Schlacher T, Richer de Forges B (2007) Seamount benthos. In: Pitcher A, Morato T, Hart PJB, Clark MR, Haggan N, Santos RS (eds) Seamounts: ecology, fisheries and conservation. Fish and Aquatic Resource Series 12. Blackwell, Oxford, p 119–140

- Seki MP, Callahan MW (1988) The feeding habits of two deep slope snappers, *Pristipomoides zonatus* and *P. auricilla*, at Pathfinder Reef, Mariana Archipelago. Fish Bull 86:807–811
- Simons RA (2011) ERDDAP—the Environmental Research Division's Data Access Program. https://coastwatch.pfeg.noaa.gov/erddap
- Stamoulis KA, Delevaux JMS, Williams ID, Poti M and others (2018) Seascape models reveal places to focus coastal fisheries management. Ecol Appl 28:910–925
- Staudigel H, Clague DA (2010) The geological history of deep-sea volcanoes: biosphere, hydrosphere, and lithosphere interactions. Oceanography 23:58–71
 - Thistle D (2003) The deep-sea floor: an overview. In: Tyler PA (ed) Ecosystems of the world. Elsevier, New York, NY, p 1–37
- Tracey DM, Bull B, Clark MR, Mackay KA (2004) Fish species composition on seamounts and adjacent slope in New Zealand waters. NZ J Mar Freshw Res 38: 163–182
- Tracey DM, Clark MR, Anderson OF, Kim SW (2012) Deepsea fish distribution varies between seamounts: results from a seamount complex off New Zealand. PLOS ONE 7:e36897

Editorial responsibility: Rebecca G. Asch, Greenville, North Carolina, USA Reviewed by: 3 anonymous referees

- Uchida RN, Uchiyama JH (eds) (1986) Fishery atlas of the Northwestern Hawaiian Islands. NOAA Tech Rep NMFS 38, US Department of Commerce. https://spo.nmfs.noaa. gov/sites/default/files/legacy-pdfs/tr38.pdf
- Victorero L, Robert K, Robinson LF, Taylor ML, Huvenne VAI (2018) Species replacement dominates megabenthos beta diversity in a remote seamount setting. Sci Rep 8:4152
 - White M, Bashmachnikov I, Aristegui J, Martins A (2007)
 Physical processes and seamount productivity. In:
 Pitcher TJ, Morato T, Hart PJB, Clark MR, Haggan N,
 Santos RS (eds) Seamounts: ecology, fisheries, and conservation. Fish and Aquatic Resource Series 12. Blackwell Publishing, Oxford, p 65–84
 - Wilson RR, Kaufman RS (1987) Seamount biota and biogeography. Geophys Monogr 43:355–377
- Wilson SK, Graham NAJ, Polunin NV (2007) Appraisal of visual assessments of habitat complexity and benthic composition on coral reefs. Mar Biol 151:1069–1076
- Yeh J, Drazen JC (2009) Depth zonation and bathymetric trends of deep-sea megafaunal scavengers of the Hawaiian Islands. Deep Sea Res I 56:251–266
- Zuur AF, Ieno EN, Elphick CS (2010) A protocol for data exploration to avoid common statistical problems. Methods Ecol Evol 1:3–14

Submitted: April 1, 2021 Accepted: April 27, 2022

Proofs received from author(s): June 21, 2022